The Journal of Experimental Biology 212, 184-193
Published by The Company of Biologists 2009
doi:10.1242/jeb.021857

Regional variation in parvalbumin isoform expression correlates with muscle performance in common carp (*Cyprinus carpio*)

Philip Brownridge[1,*], Luciane Vieira de Mello[2,*], Mary Peters[1,*], Lynn McLean[1], Amy Claydon[1], Andrew R. Cossins[2], Phillip D. Whitfield[1] and Iain S. Young[1,†]

[1]Faculty of Veterinary Science and [2]School of Biological Sciences, University of Liverpool, Liverpool, UK

*These authors contributed equally to this work
†Author for correspondence (e-mail: isyoung@liverpool.ac.uk)

Accepted 3 November 2008

SUMMARY

The mechanical properties of the axial muscles vary along the length of a fish's body. This variation in performance correlates with the expression of certain muscle proteins. Parvalbumin (PARV) is an important calcium binding protein that helps modulate intracellular calcium levels which set the size and shape of the muscle calcium transient. It therefore has a central role in determining the functional properties of the muscle. Transcript data revealed eight specific isoforms of PARV in common carp (*Cyprinus carpio*) skeletal muscle which we classified as α1 and β1–7. This study is the first to show expression of all eight skeletal muscle PARV isoforms in carp at the protein level and relate regional differences in expression to performance. All of the PARV isoforms were characterised at the protein level using 2D-PAGE and tandem mass spectrometry. Comparison of carp muscle from different regions of the fish revealed a higher level of expression of PARV isoforms β4 and β5 in the anterior region, which was accompanied by an increase in the rate of relaxation. We postulate that changes in specific PARV isoform expression are an important part of the adaptive change in muscle mechanical properties in response to varying functional demands and environmental change.

Key words: muscle, parvalbumin, isometric force, activation, relaxation, proteomics, swimming.

INTRODUCTION

Muscles power a huge diversity of activities requiring a wide range of mechanical properties; however, our understanding of the molecular mechanisms underlying these properties is incomplete. The proteins involved in Ca^{2+} handling play a central role in determining the properties of muscle. These include the ion channels and pumps in the cell membrane and sarcoplasmic reticulum (SR) that control the release and reuptake of Ca^{2+}; troponin-C, which modulates the effect of Ca^{2+} on the contractile proteins; and the Ca^{2+} binding proteins, of which the most significant is parvalbumin (PARV). PARV is a small (~12 kDa) sarcoplasmic protein that plays a key role in muscle relaxation (Lannergren et al., 1993; Muntener et al., 1995; Jiang et al., 1996; Baylor and Hollingworth, 1998; Vornanen et al., 1999), acting as an intracellular Ca^{2+} buffer to determine the duration and magnitude of the activating Ca^{2+} signal (Wnuk et al., 1982; Pauls et al., 1996) and thus the force and duration of contraction. This role is highlighted by the fact that PARV permits muscle relaxation in the absence of all other Ca^{2+} sequestration mechanisms (Jiang et al., 1996). Further, experimental transfection of PARV cDNA into mammalian slow-twitch fibres, which normally contain little or no PARV, dramatically increases their relaxation rate (Muntener et al., 1995); correspondingly, PARV knockout mouse fast-twitch muscle has slower Ca^{2+} transients and relaxation rates than wild-type (Schwaller et al., 1999).

The mechanical properties of the axial muscles vary along the length of a fish's body (Altringham et al., 1993; Davies et al., 1995; Swank et al., 1997; Ellerby and Altringham, 2001). These regional differences correlate with changes in the expression of various muscle proteins including PARV (Thys et al., 1998; Thys et al., 2001). Previous studies typically only identified small numbers of PARV isoforms and, therefore, focused on correlating muscle performance with total PARV expression. Whilst mammalian species typically have two isoforms of PARV, α and β, fish often possess many isoforms. Transcript analysis of zebrafish (*Danio rerio*) identified nine isoforms of PARV (Friedberg, 2005) and five PARV isoforms have previously been identified in common carp (*Cyprinus carpio*) (Coffee and Bradshaw, 1973).

We employed an integrative strategy to explore the molecular mechanisms underlying muscle function. We used transcriptomic and proteomic strategies to identify and characterise multiple isoforms of PARV in the fast-twitch axial muscle from anterior and posterior regions of common carp. We also measured the mechanical properties of the muscle in terms of activation and relaxation times and contractile force. This allowed us to relate the differential expression of the PARV isoforms to muscle performance, helping to bridge the intellectual gap between protein expression and functional properties.

MATERIALS AND METHODS

Our experimental strategy is shown in Fig. 1. The biochemical aspect investigated changes in PARV expression, which can vary in two ways: firstly in the total amount of PARV expressed and secondly in the composition of the isoforms. These were analysed separately: changes in total PARV expression were analysed by 1D-SDS-PAGE and PARV isoform composition was analysed by 2D-PAGE. Muscle mechanical properties were determined in terms of activation and relaxation times for twitch contractions and maximum isometric force during a supramaximal tetanic contraction.

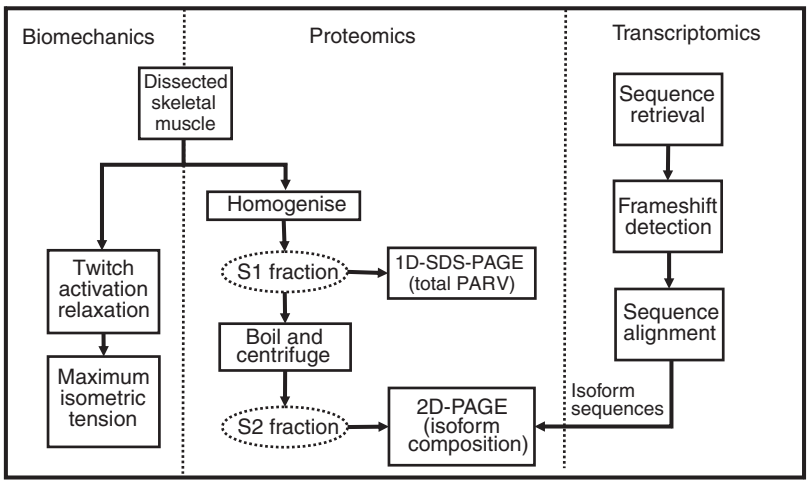

Fig. 1. The different analyses performed. Transcript and protein level analyses were employed to detect and characterise PARV isoforms, and biomechanics was used to quantify the physiological outputs.

Sequence analysis

The carp database (carpBase) is available at http://legr.liv.ac.uk. All the expressed sequence tag (EST) sequences with a BlastX hit for PARV were retrieved, making a total of 122 transcript sequences. For apparently incomplete protein sequences, possible frame shifts were investigated using the translate tool at the Expasy website (http://www.expasy.org/tools/dna.html). Only sequences that could be unambiguously completed in this way were considered for further analysis. Remaining clones with partial sequences were not considered in further analyses. The protein sequences were aligned using ClustalW (Thompson et al., 1994). Manipulation of alignments was performed with Jalview (Clamp et al., 2004). The consensus sequences for the PARV groups determined by the alignment were obtained using Jemboss v1.3 (Carver and Bleasby, 2003). Because of the relatively high error rate associated with ESTs, we required each cluster to have at least four sequences. The nomenclature applied to our consensus isoform sequences followed the α/β classification (Hsiao et al., 2002; Henzl et al., 2004) and was informed by phylogenetic analysis (data not shown). A consensus, neighbour-joining phylogenetic tree was constructed and drawn with the PHYLIP package (Felsenstein, 1989). Branch support was evaluated by 1000 bootstrap replicates.

Dissection of carp skeletal muscle

Common carp (*Cyprinus carpio*, Linnaeus 1758) were purchased from Rodbaston College (Penkridge, Staffordshire, UK), maintained at 20°C on a 16 h light:8 h dark photoperiod and fed commercial carp pellets *ad libitum*. The fish were killed by stunning with a sharp blow to the head and swiftly double-pithed in accordance with local and Home Office Schedule One approved protocols.

Three strips of skeletal muscle, 3 mm wide and approximately 2 mm deep, running from the opercular flap to the caudal peduncle, were cut from the right-hand side axial muscle using a multi-bladed tool. Samples were taken from fish of similar age (1 year). Their mass was 235±68 g and length was 242±27 mm (means ± s.d.). For biomechanics experiments, the strips were pinned out in oxygenated Ringer solution (132 mmol l^{-1} NaCl, 2.6 mmol l^{-1} KCl, 10 mmol l^{-1} imidazole, 1 mmol l^{-1} $MgCl_2$, 10 mmol l^{-1} pyruvate, 2.7 mmol l^{-1} $CaCl_2$) and left to recover before further processing. For biochemical analysis the whole region of dorsal axial white muscle was dissected from the left-hand side of the fish and divided into 'anterior' from the opercular flap to 0.3 body lengths down the fish, 'middle' from 0.3 to 0.7 body lengths and 'posterior' from 0.7 body lengths to the tail. These were then chopped into approximately 1 cm cubes, placed into labelled 1.5 ml snap-top vials and frozen at –80°C.

Sample preparation for proteomic analyses

Muscle samples (approximately 250 mg) were mechanically homogenised in 2.5 ml of 20 mmol l^{-1} sodium phosphate buffer (pH 7.4) containing Complete Protease Inhibitors (Roche, Lewes, UK). The homogenate was centrifuged at 12,500 ***g*** at 4°C for 45 min and the supernatant removed and set aside. The remaining pellet was re-suspended in 1 ml of homogenisation buffer, re-homogenised, centrifuged and the supernatant combined with the supernatant set aside in the previous step. This combined supernatant was then divided into two aliquots. One aliquot (S1) was stored at –20°C and used for determination of total PARV by 1D-SDS-PAGE. The second aliquot was used for PARV isoform analysis by 2D-PAGE. This second aliquot was heated at 95°C for 5 min and then centrifuged for 10 min at 14,000 ***g***. The resulting supernatant (S2) was stored at –20°C. The protein concentration of the unboiled and boiled fractions was determined using the Coomassie Plus Protein Assay (Pierce Biotechnology, Rockford, IL, USA).

PARV expression can differ either by a change in the total amount of PARV expressed or by a change in the composition of the PARV isoforms. Both of these attributes were analysed to determine the difference in PARV expression between posterior and anterior fast-twitch muscle. A 2D-PAGE approach was required to analyse the differences in PARV isoform composition. In order to detect low abundance isoforms, a PARV-enriched fraction was prepared by boiling the homogenate and it was then subjected to 2D-PAGE. PARV is thermostable and boiling is a well established procedure to produce a fraction highly enriched in PARV (Pechere et al., 1971). Taking this into consideration the muscle homogenate was boiled for 5 min. Following centrifugation of the boiled material the supernatant contained a relatively pure preparation of PARV. To ensure that this boiling did not affect the isoform composition, selected unboiled samples were run under the 2D-PAGE protocol. Allowing for loading differences, a similar isoform composition was observed (data not shown) with high abundance isoforms present in similar composition but with lower abdundance isoforms missing. It is difficult to determine changes in total PARV concentration from a boiled sample, so total PARV expression was investigated by 1D-SDS-PAGE of the soluble fraction of the fast-twitch muscle homogenate. The use of an unboiled sample allows PARV concentration to be expressed as a fraction of the total protein. To compensate for biological variation,

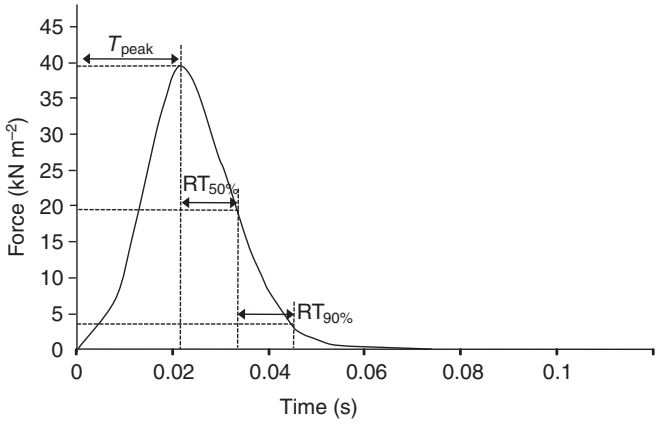

Fig. 2. A typical twitch record, chosen as it has kinetics close to the mean values obtained. Time to peak twitch tension T_{peak} was measured as the time from baseline force to peak force during activation. The time taken for the muscle force to decline from its peak to 50% of its peak ($RT_{50\%}$) and to 10% of its peak (i.e. a 90% decline in force; $RT_{90\%}$) were used as indices for the rate of relaxation.

anterior and posterior samples were taken from six fish and analysed for total PARV expression and isoform composition.

1D gel electrophoresis

The soluble muscle proteins from the unboiled fraction were separated by 1D-SDS-PAGE using a Mini-Protean 3 system (Biorad Laboratories Ltd, Hemel Hempstead, Herts, UK). Muscle samples (5 µg) were electrophoresed at a constant potential of 200 V through a 15% w/v resolving gel with a 4% w/v stacking gel. Samples were heated at 95°C for 5 min in a reducing buffer [125 mmol l^{-1} Tris-HCl, 140 mmol l^{-1} SDS, 20% v/v glycerol, 200 mmol l^{-1} dithiothreitol (DTT) and 30 mmol l^{-1} Bromophenol Blue] prior to loading. Gels were stained with Coomassie Blue stain (Candiano et al., 2004).

2D gel electrophoresis

Soluble extracts of the boiled homogenates were analysed by 2D-PAGE using a 24 cm pH 4–5 immobilised pH gradient (IPG) strip in the first dimension (GE Healthcare Life Sciences, Amersham, Bucks, UK). The samples (500 µg) were mixed with five volumes of ice-cold acetone and held at –20°C for 1 h. They were centrifuged at 5000 ***g*** for 5 min, the excess acetone was removed and the samples were dried in an oven at 37°C for 10 min. The pellets were resuspended in buffer containing CHAPS (4% w/v), 7 mol l^{-1} urea, 20 mmol l^{-1} DTT and ampholytes (0.5% v/v) on a shaker for 1 h, then centrifuged at 8000 ***g*** for 5 min. The IPG strips were loaded face-down into an IPGPhor unit (GE Healthcare Life Sciences) and rehydrated (12 h at 30 V, 20°C) followed by isoelectric focusing (1 h at 500 V, 1 h at 1000 V and 96,000 Vh at 8000 V). The focused IPG strips were equilibrated in 50 mmol l^{-1} Tris-HCl, pH 8.8, containing 6 mol l^{-1} urea, 30% v/v glycerol, 2% w/v SDS, with a trace of Bromophenol Blue. DTT (10 mg ml^{-1}) was present as a reducing agent for the initial equilibration. A second equilibration step was carried out with iodoacetamide (25 mg ml^{-1}) present in place of DTT. The IPGs were then run out on a 15% acrylamide gel. The gels were stained overnight in colloidal Coomassie stain (Candiano et al., 2004) and destained in water for a further 24 h.

Gel image analysis

1D-SDS-PAGE gels were scanned at 600 d.p.i. and the images analysed using ImageJ (W. S. Rasband, ImageJ, U.S. National Institutes of Health, Bethesda, MD, USA, http://rsb.info.nih.gov/ij/, 1997-2008). 2D-PAGE gels were scanned at 600 d.p.i. and the images analysed using Phoretix 2D Evolution Software (version 2004; Nonlinear Dynamics, Newcastle upon Tyne, UK). Paired *t*-tests were carried out using Statsdirect (version 2.6.2) software (StatsDirect, Altrincham, Cheshire, UK). The results of the *t*-tests were modified by the Bonferroni correction to adjust for the multiple significance testing (Bland and Altman, 1995).

In-gel tryptic digestion

Gel plugs were manually excised with a 5 ml plastic pipette and incubated with destain solution (acetonitrile:100 mmol l^{-1} ammonium bicarbonate, 50:50) at 37°C for 10 min. This process was repeated until all the stain had been removed. Each gel plug was then dehydrated by incubation with acetonitrile at 37°C for 10 min. The acetonitrile was removed and the plug dried in a vacuum centrifuge for 1 h. The gel was rehydrated with 12.5 ng µl^{-1} trypsin (Roche) in 50 mmol l^{-1} ammonium bicarbonate. After 30 min, 50 mmol l^{-1} ammonium bicarbonate was added to each sample, and digestion was allowed to continue overnight at 37°C. The digestion was terminated by the addition of 10% formic acid. The digests were then desalted with StageTips (Proxeon Biosystems, Odense, Denmark) using a binding/washing solution of 5% formic acid and eluting in 5% formic acid in 50:50 acetonitrile:water.

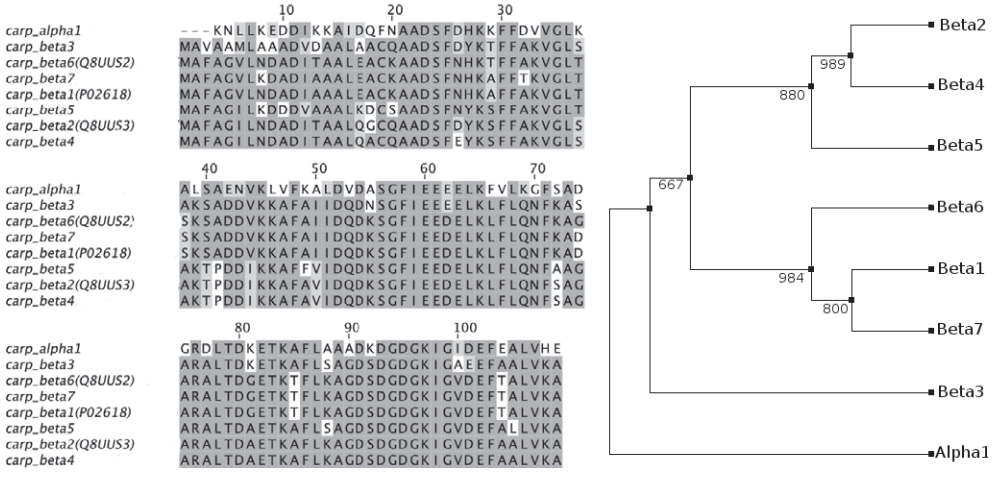

Fig. 3. A sequence consensus alignment for all the parvalbumin genes from the carpBase database (120 transcripts). The phylogenetic connection between the isoforms alongside their theoretical physical properties is also shown. The figure was made with Jalview (www.ebi.ac.uk/~michele/jalview) and a consensus, neighbour-joining phylogenetic tree illustrating the relationship between the isoforms [drawn with the PHYLIP package (Felsenstein, 1989)].

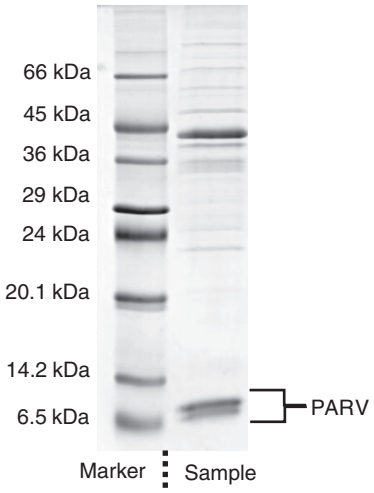

Fig. 4. A 15% 1D-SDS-PAGE gel of the unboiled soluble fraction of fast-twitch muscle.

MALDI–TOF mass spectrometry analysis

MALDI–TOF MS (matrix assisted laser desorption ionisation–time of flight mass spectrometry) analysis was performed using a Micromass M@LDI (Waters, Manchester, UK). Peptide samples were mixed 1:1 with 10 mg ml^{-1} α-cyano-4-hydroxycinnamic acid in 50:50 acetonitrile:water 0.1% (v/v) trifluoroacetic acid and 1 µl of the resulting mixture was spotted onto a MALDI target. The calibration was based on the monoisotopic masses of a mixture of standard peptides: des-Arg$_1$ bradykinin (mass to charge ratio, *m/z* 904.47), angiotensin II (*m/z* 1046.51), angiotensin I (*m/z* 1296.99), neurotensin (*m/z* 1672.92), ACTH fragment 18–39 (*m/z* 2318.30) and insulin B chain (*m/z* 3494.65). All standards were purchased from Sigma (Poole, Dorset, UK). Spectra were collected in positive ion mode over the range *m/z* 800–4000.

Peptide sequencing by ESI–MS/MS

ESI–MS/MS (electrospray ionisation–tandem mass spectrometry) was performed using a Q-TOF Micro (Waters). Spectra were collected in positive ion mode. The samples were loaded into borosilicate nanospray needles, which were either gold coated (Waters) or platinum coated (Proxeon Biosystems). Spray was initiated by applying a capillary voltage of 800–1200 V and stabilised by a small amount of back-pressure provided by nitrogen gas. The product ion spectrum from human [Glu$_1$]-fibropeptide B (M_r 1570.62, Sigma) was used as the mass calibrant. Doubly or triply charged peptide ions were identified from a survey scan (*m/z* 400–2000), following which individual precursor ions were manually selected for fragmentation. The collision energy was determined manually and argon was used as the collision gas at a pressure of 15 p.s.i. (103.4 kPa). The resulting product data were manually interpreted.

PARV isoform identification

MALDI–TOF and ESI–MS/MS data were searched using an in-house installation of Mascot (Perkins et al., 1999) searching against a customised database of carp cDNA sequences extracted from carpBase (Gracey et al., 2004). The parameters used were as follows: trypsin allowing for four missed cleavages, carbamidoalkylation modification of cysteine residues as a fixed modification and protein N-terminal acetylation as a variable modification. Mass accuracy was selected to be within 50 p.p.m.

Preparation of samples for biomechanics

The quality of the longitudinal muscle strips (see above) was determined by causing them to twitch using electrical stimulation (130 V for 2 ms at 1 Hz). Strips that failed to twitch vigorously were immediately rejected. Muscle preparations of less than 1 mm diameter, encompassing one myotome and preserving myosepta at each end, were dissected. These preparations were tied by the myosepta at each end with no. 6 silk suture thread and allowed to recover in cool (4°C) oxygenated Ringer solution.

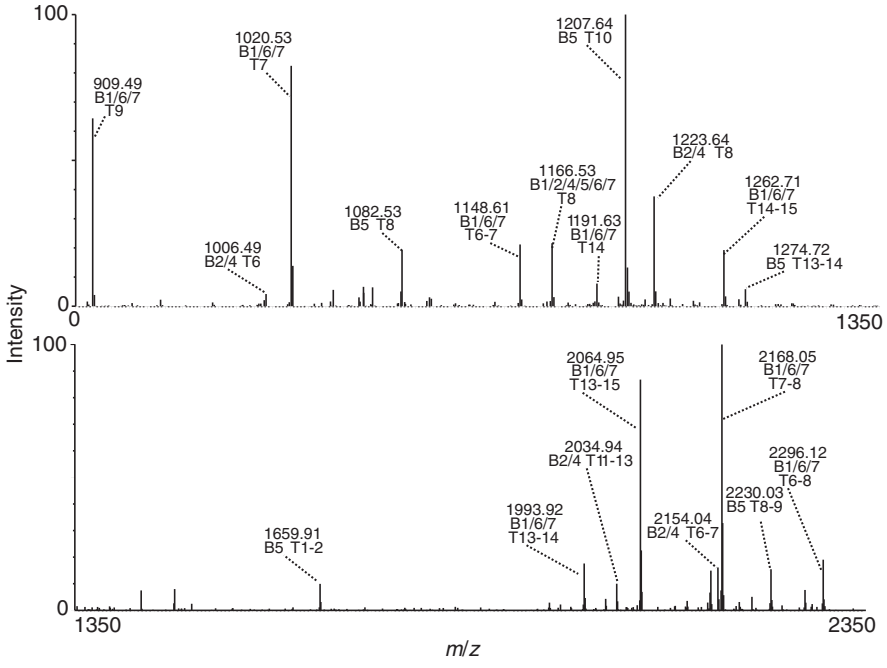

Fig. 5. MALDI–TOF (matrix assisted laser desorption ionisation–time of flight) mass spectrum of an in-gel tryptic digestion of the band corresponding to PARV from a 1D-SDS-PAGE of the unboiled soluble fraction of fast-twitch muscle. Proposed peak identities are shown in Table 1.

Table 1. Proposed identities of the peaks from MALDI–TOF mass spectrometry of in-gel tryptic digestions of the band corresponding to PARV from a 1D-SDS-PAGE of the unboiled soluble fraction of fast-twitch muscle (see Fig. 4)

PARV β1: mass, 11486; score, 113; expect, 1.8e–007; queries matched, 10; frame, 1

Observed	M_r (expt)	M_r (calc)	Delta	Start	End	Miss	Peptide
909.49	908.48	908.51	–0.03	65	71	0	K.LFLQNFK.A
1020.53	1019.52	1019.53	–0.01	46	54	0	K.AFAIIDQDK.S
1148.61	1147.60	1147.62	–0.02	45	54	1	K.KAFAIIDQDK.S
1166.53	1165.52	1165.55	–0.03	55	64	0	K.SGFIEEDELK.L
1191.63	1190.62	1190.65	–0.03	97	107	0	K.IGVDEFTALVK.A
1262.71	1261.70	1261.69	0.01	97	108	1	K.IGVDEFTALVKA.–
1993.92	1992.91	1992.96	–0.05	88	107	1	K.AGDSDGDGKIGVDEFTALVK.A
2064.95	2063.94	2064.00	–0.06	88	108	2	K.AGDSDGDGKIGVDEFTALVKA.–
2168.05	2167.04	2167.07	–0.03	46	64	1	K.AFAIIDQDKSGFIEEDELK.L
2296.12	2295.11	2295.16	–0.05	45	64	2	K.KAFAIIDQDKSGFIEEDELK.L

PARV β5: mass, 11528; score, 72; expect, 0.0025; queries matched, 7; frame, 1

Observed	M_r (expt)	M_r (calc)	Delta	Start	End	Miss	Peptide
1082.53	1081.52	1081.54	–0.02	46	54	0	K.AFFVIDQDK.S
1166.53	1165.52	1165.55	–0.03	55	64	0	K.SGFIEEDELK.L
1203.68	1202.67	1202.69	–0.02	97	107	0	K.IGVDEFALLVK.A
1207.64	1206.63	1206.65	–0.02	65	75	0	K.LFLQNFAAGAR.A
1274.72	1273.71	1273.73	–0.02	97	108	1	K.IGVDEFALLVKA.–
1659.91	1658.90	1658.89	0.01	1	16	1	N–Acetyl–AFAGILKDDDVAAALK.D
2230.03	2229.02	2229.08	–0.06	46	64	1	K.AFFVIDQDKSGFIEEDELK.L

PARV β2: mass, 11423; score, 49; expect, 0.46; queries matched, 5; frame, 1

Observed	M_r (expt)	M_r (calc)	Delta	Start	End	Miss	Peptide
1006.49	1005.48	1005.51	–0.03	46	54	0	K.AFAVIDQDK.S
1166.53	1165.52	1165.55	–0.03	55	64	0	K.SGFIEEDELK.L
1223.64	1222.63	1222.65	–0.01	65	75	0	K.LFLQNFSAGAR.A
2034.94	2033.93	2033.99	–0.06	88	108	2	K.AGDSDGDGKIGVDEFAALVKA.–
2154.04	2153.03	2153.05	–0.02	46	64	1	K.AFAVIDQDKSGFIEEDELK.L

PARV, parvalbumin; MALDI, matrix assisted laser desorption ionisation; TOF, time of flight.

Biomechanics

For the mechanical measurements, the preparations were transferred to a flow-through chamber circulated with oxygenated Ringer solution maintained at 20°C. One end was tied to the hook of a model 308B high-speed length controller (Aurora Scientific, Aurora, Canada) and the other was tied to a hook secured to a model 31 force transducer and S7DC amplifier (RDP, Wolverhampton, UK). The muscle was stimulated using single square-wave electrical pulses (2 ms), peak force per twitch was determined and the length was varied to yield a maximum peak force. Three twitches were performed at this optimum length and the contraction and relaxation periods averaged (Fig. 2). A maximum isometric tetanus was elicited and stimulation frequency was optimised to produce maximum tetanic force (stimulus train duration 300 ms, stimulation frequency 150 Hz) to measure maximum isometric force production. So that we could calculate muscle stress, at the end of the experiment the preparations were blotted gently on absorbent paper then weighed. Cross-sectional area was calculated as the wet preparation mass (kg) divided by 1060 to give the volume (m^3), then the volume was divided by the muscle fibre length, measured at the peak of the length–tension curve using a calibrated eyepiece graticule.

RESULTS

Identification of PARV isoforms at the transcript level

Eight different groups were identified after a protein sequence alignment of all the translated carpBase PARV transcript sequences, showing that there are at least eight different PARV isoforms in common carp. An extensive literature search revealed widespread confusion in PARV nomenclature. A rigorous phylogentic analysis based on the PARV sequences currently held in the SwissProt and Trembl databases, supplemented with our carp sequences and annotated PARV sequences from the completed genomes of fugu (Clark et al., 2003) and zebrafish (Friedberg, 2005), revealed many inconsistencies in the zebrafish and fugu nomenclature. However, the traditional nomenclature for PARVs, based on the division of the α- and β-type isoforms by their biochemical properties, chiefly that β-forms have an isoeletric point of less than five and a cysteine at position 18, produced clusters of carp EST sequences which we named carp_α1, carp_β1, carp_β2, carp_β3, carp_β4, carp_β5, carp_β6 and carp_β7. The aligned consensus sequences for each of the groups are shown in Fig. 3.

Identification of expressed parvalbumin isoforms

The transcript data only have functional relevance in living tissues if it can be demonstrated that the protein products are expressed. We therefore undertook studies to analyse the specific PARV isoforms. The soluble muscle proteins were initially separated by 1D-SDS-PAGE (Fig. 4). This analysis revealed a large dynamic range in protein expression, with the distributions and intensities of protein bands similar to those described in the skeletal muscle of other fish species (Verrez-Bagnis et al., 2001; Winnard et al., 2003; Grzyb and Skorkowski, 2005; McLean et al., 2007). PARV appears as two narrowly spaced bands on the 1D-SDS-PAGE of the soluble fraction (S1) of fast-twitch muscle homogenate (Fig. 4). The bands migrate between 6.5 and 14.2 kDa, which corresponds to the theoretical molecular mass of PARV (~12 kDa). PARV is found in high concentrations in fast-twitch skeletal muscle and accounts for the second-most intense band in the gel. In-gel tryptic digestion and MALDI–TOF MS analysis revealed that these bands contain a mixture of PARV isoforms (Fig. 5). The high sequence homology between PARV isoforms results in many common peptides so it is impossible to distinguish individual isoforms; thus only broad groups can be identified based on their shared peptides: β1/β6/β7, β5 and β2/β4 (Table 1 and Fig. 6).

To overcome this problem 2-D PAGE was used to enhance separation of the individual PARV isoforms. Despite the small differences in the predicted pI values of the PARV isoforms, the availability of micro-range IPG strips, which span a single pH unit, enabled the successful resolution of the isoforms (Fig. 7). All eight isoforms identified from the transcript analysis were observed and were located along the horizontal axis in the order predicted from theoretical pI calculations. The proteins present in the gel spots were identified using ESI–MS/MS. *De novo* sequencing was targeted by the transcript analysis, which revealed that each PARV isoform yielded a unique N-terminal tryptic peptide. This N-terminal sequencing allowed unambiguous identification of the protein spots. The sequencing confirmed the removal of the initiator methionine and indicated that the isoforms were naturally N-acetylated. The

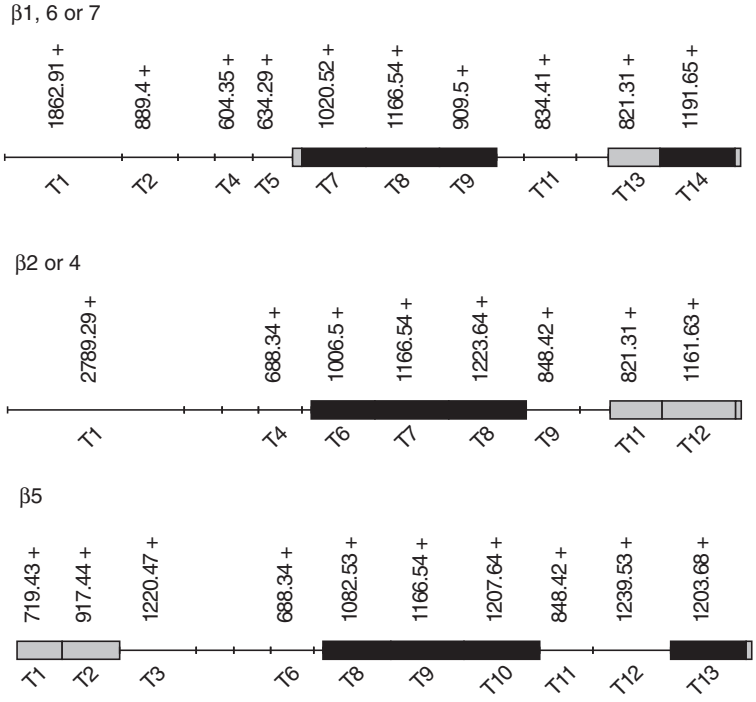

Fig. 6. Peptide maps representing the peptides observed by MALDI–mass spectrometry (MS) of the in-gel tryptic digestion of the band corresponding to PARV from a 1D-SDS-PAGE of the unboiled soluble fraction of fast-twitch muscle (see Fig. 5). The black regions indicate that the peptide is observed and the light grey regions indicate that the peptide is observed as part of a missed cleavage. Figure produced using PeptideMapper (Beynon, 2005).

isoforms were expressed in different abundances: isoforms β1, β2, β6 and β7 had the highest expression levels, isoforms β4 and β5 were present in lower amounts whilst isoforms α and β3 were at the detection limit of the analysis. The α isoform was found at such low abundance that identification required spots to be pooled from multiple gels.

Regional variation in total PARV expression

1D-SDS-PAGE with scanning densitometry of the gels to determine the concentration of total PARV in relation to total soluble protein revealed that the anterior of the fish had significantly higher levels of PARV expression than the posterior (Table 2). The paired *t*-test revealed a two-sided *P* value of 0.0006, which also remained significant after Bonferroni correction (Table 2).

PARV isoform composition was measured with 2D-PAGE by determining the spot volume corresponding to each protein as a fraction of the total integrated spot density on the gel. The 24 cm micro-range IPG strip provided sufficient resolution to fully resolve all the PARV isoforms (Fig. 8). Isoforms β4 and β5 constitute a significantly greater proportion of cellular PARV in the anterior of the fish compared with the posterior of the fish (paired *t*-test; Table 3). In contrast, the proportion of cellular PARV corresponding to isoforms β1 and β6 decreased significantly, whilst β2 showed no significant difference.

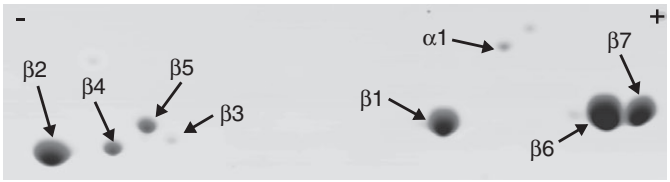

Fig. 7. The cropped region of a 15% 2D-PAGE gel displaying the separation of PARV isoforms by a 24 cm, pH 4–5 immobilised pH gradient (IPG) strip. The spots were identified by in-gel tryptic digestion followed by nanospray-tandom mass spectrometry (MS/MS) sequencing of the N-terminal peptides (except for α, which was identified from the C-terminus).

Biomechanics

The maximum tetanic stress measured in posterior preparations was 39.2±18.6 kN m^{-2} (mean ± s.e.m.), significantly higher (two-sided, paired *t*-test, $P<0.05$, $N=11$) than that generated by anterior preparations (18.1±11.4 kN m^{-2}; Fig. 9). These stresses are comparatively low; however, our calculation of muscle cross-sectional area is likely to be an overestimate as it is derived from preparation mass without correction for substantial amounts of connective tissue in the myosepta and the remains of cut fibres still attached to the myosepta. The anterior preparations were significantly faster as demonstrated by significantly shorter activation times (two-sided, paired *t*-test, $P<0.05$, $N=8$): time to peak

Table 2. The densitometry results from analysis of the soluble fraction of fast-twitch muscle by 15% 1D-SDS-PAGE

Sample	% PARV	% increase in anterior	Paired *t*-test
11/12/06A back	20.0		*P*:
11/12/06A front	23.9	19.4	0.0006
11/12/06B back	13.1		
11/12/06B front	15.7	19.5	
13/12/06A back	23.9		
13/12/06A front	25.9	8.1	
13/12/06B back	19.1		
13/12/06B front	21.3	11.2	Bonferroni correction:
16/01/06A back	20.3		0.0048
16/01/06A front	27.2	34.0	
16/01/06B back	16.6		
16/01/06B front	24.1	45.6	
5/12/06A back	22.0		
5/12/06A front	27.0	22.8	
6/12/06A back	13.0		
6/12/06A front	18.7	44.3	

In order to minimize the contribution of sample loading variations, the changes in PARV expression were determined by calculating the ratio of the peak area of the PARV band against the combined peak area for the whole lane.

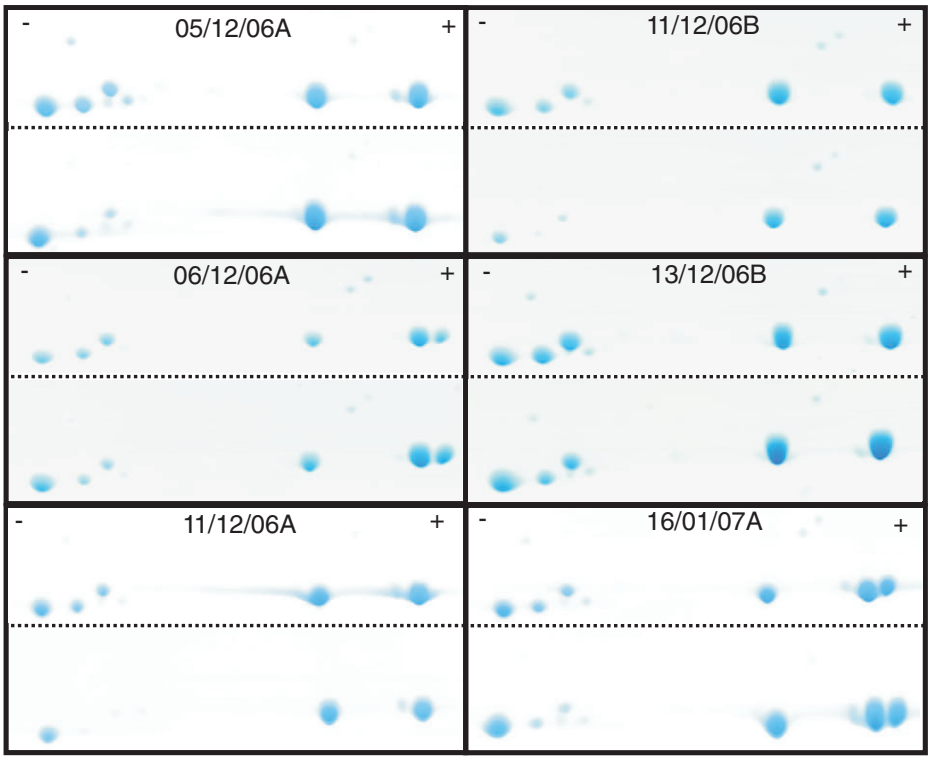

Fig. 8. Cropped regions of 2D-PAGE using a 24 cm IPG strip of boiled sample showing the difference between the anterior (top image in each frame) and posterior (lower image in each frame) areas of the fish.

Table 3. The densitometry results from analysis of the soluble fraction of fast-twitch muscle by 2D-PAGE using a 24 cm, pH4–5 IPG (see Fig. 8)

Isoform	Sample	% posterior	% anterior	Change	*t*-test	Bonferroni
β1	06/12/06A	17.36	15.48	–1.88	0.008	0.046
	11/12/06B	39.06	32.07	–6.99		
	13/12/06B	30.84	24.30	–6.54		
	5/12/06A	28.13	25.87	–2.26		
	11/12/06A	38.52	36.34	–2.17		
	16/01/06A	20.45	16.07	–4.38		
β2	06/12/06A	17.11	14.64	–2.47	0.830	4.978
	11/12/06B	13.37	18.35	4.98		
	13/12/06B	19.50	17.78	–1.72		
	5/12/06A	11.40	13.88	2.48		
	11/12/06A	15.00	11.88	–3.12		
	16/01/06A	13.52	15.16	1.65		
β4	06/12/06A	4.15	8.81	4.66	0.001	0.008
	11/12/06B	0.23	8.47	8.24		
	13/12/06B	7.16	14.57	7.41		
	5/12/06A	3.94	10.68	6.74		
	11/12/06A	2.50	4.61	2.11		
	16/01/06A	2.84	8.62	5.78		
β5	06/12/06A	5.33	11.55	6.22	<0.001	<0.001
	11/12/06B	3.18	9.97	6.79		
	13/12/06B	10.67	15.98	5.31		
	5/12/06A	3.13	12.52	9.39		
	11/12/06A	0.00	6.67	6.67		
	16/01/06A	4.37	11.90	7.54		
β6	06/12/06A	33.75	33.33	–0.42	0.019	0.115
	11/12/06B	44.16	31.13	–13.03		
	13/12/06B	31.84	27.36	–4.48		
	5/12/06A	15.81	8.70	–7.11		
	11/12/06A	43.98	40.50	–3.48		
	16/01/06A	58.82	48.25	–10.57		

Isoforms α, β3 and β7 have been excluded from the table because they were not present on all gels.

twitch tension was 20.7±1.0 ms compared with 25.4±1.1 ms in the posterior. Similarly, the rate of relaxation was significantly higher in the anterior preparations; Fig. 10). The time taken for the force to fall to 50% of the peak value (16.0±3.0 ms *vs* 23.9±5.0 ms) and the time from peak force to 10% of the peak value, which we termed 90% relaxation (28.5±4.0 ms *vs* 47.1±7.5 ms) were significantly shorter (two-sided, paired *t*-test, $P<0.05$, $N=8$) in the anterior.

DISCUSSION

Systems biology promotes an integrative approach, applying molecular, genetic, cellular and functional information to reveal how the whole organism works. These studies highlight the complexity of inter-relating mechanisms and molecular associations in a living organism and offer the possibility of bridging the gap between genome and phenotype. This study was driven by the discovery that the fish muscle transcriptome codes for multiple PARV isoforms, and that the transcription of these isoforms changes under different functional demands (Gracey et al., 2004). While it is well known that the total amount of PARV plays a major role in the relaxation kinetics of muscle, the significance of the mix of isoforms expressed remains largely unexplored. Taking into consideration the fact that muscle properties and total PARV expression vary along the length of the fish (Thys et al., 1998; Thys et al., 2001) we

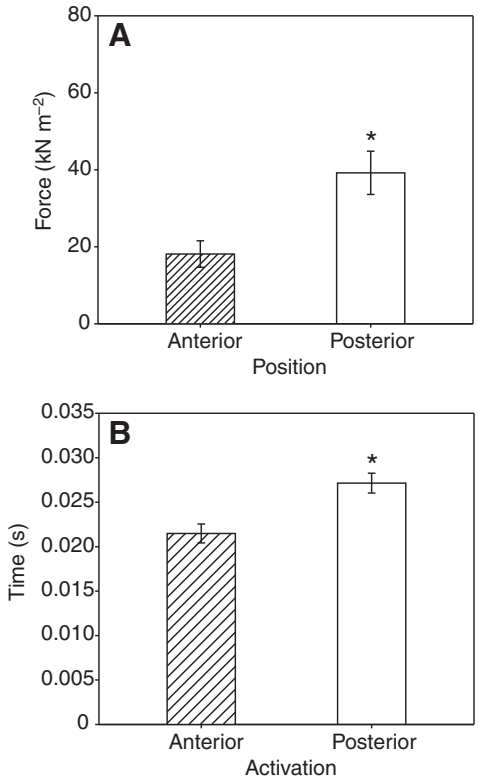

Fig. 9. Mechanical properties of the anterior and posterior axial muscles: maximum isometric force and activation. Error bars are ±s.e.m. (A) Maximum isometric force measured during a tetanic contraction. (B) Activation measured as the time from zero force to the peak twitch force. *P<0.05.

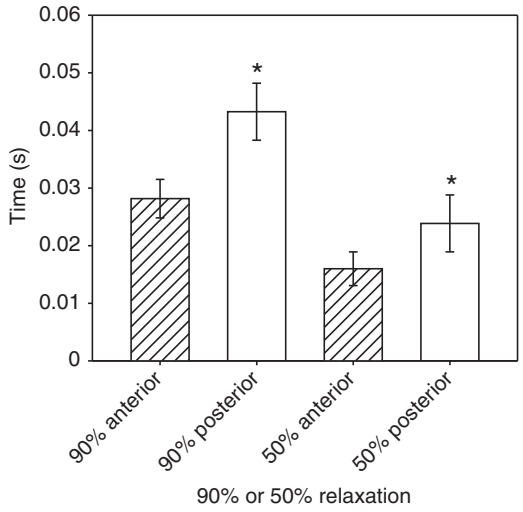

Fig. 10. Mechanical properties of the anterior and posterior axial muscles: relaxation kinetics. Error bars are ±s.e.m. The graph shows time to 90% maximum force (left) and 50% maximum force (right) during the relaxation phase. *P<0.05.

supposed that PARV isoform expression might correlate with muscle location and mechanical performance. We set out to test this hypothesis.

Our transcript analysis revealed that carp, like zebrafish (Friedberg, 2005), possess a high number of β isoforms and a low number of α isoforms of PARV. This similarity to zebrafish is extended in so far as there are clear subclades within the β PARV family. While previous studies have described only four (Brandts et al., 1977) or five (Pechere et al., 1971; Coffee et al., 1974) PARV isoforms in carp, the increased resolution in our study achieved by 2D-PAGE with micro-range IPG strips allowed us to separate all eight PARV isoforms. By combining this with protein sequence information from tandem mass spectrometry analysis we were able to determine the identity of each PARV isoform predicted by the transcript analysis. This peptide-level identification strategy was successful where a protein-level approach would have been hindered by the close mass similarity of the isoforms.

These identifications, where data are available, agree with earlier studies: Coffee and colleagues (Coffee et al., 1974) published sequences for PARV isoforms that are identical to our β1, β2 and β6 isoforms. We found that the PARV isoforms are present in different amounts, with isoforms β1 and β6 being the most abundant. These isoforms share a subclade with β7 (Fig. 3) and represent 60% of the total PARV. The subclade β2/4 accounts for a further 20% and the more distantly related isoforms, α, β3 and β5, are present in lower amounts.

Previous studies have shown higher concentrations of PARV in the anterior axial muscle of some fish (Thys et al., 2001). Our study shows that the anterior skeletal muscle of carp does have significantly more PARV than posterior muscle by a similar magnitude to that reported by Thys and colleagues for fast-twitch muscle from wide-mouthed bass (Thys et al., 2001). Earlier studies have also found regional differences in PARV isoform composition in fast-twitch muscle in some fish species: brook trout (Coughlin et al., 2007), barbel (Huriaux et al., 1997), largemouth bass (Thys et al., 2001), sheepshead and kingfish (Wilwert et al., 2006). Our study expands on these earlier studies by examining a complete set of PARV isoforms, in turn, revealing a more complicated pattern of changes including increasing and decreasing expression with significantly higher proportions of β4 and β5 and significantly lower amounts of β1 in anterior compared with posterior muscle. This isoform shift correlates with the muscle properties. We found twitch contraction and relaxation times were significantly shorter in the anterior region of the fish and that significantly higher forces were generated in the posterior region of the fish. The faster twitch activation and relaxation kinetics in the anterior region agrees with previous work on other species: blue fin tuna (Wardle et al., 1989), saithe (Altringham et al., 1993), atlantic cod (Davies et al., 1995), largemouth bass (Thys et al., 2001) and rainbow trout (Coughlin et al., 2007).

For the muscle to produce maximum work it must relax fully between each contraction, thus minimising the work performed on the muscle during re-lengthening [often termed ‘negative work’ (e.g. Altringham and Ellerby, 1999)]. It is well known that the amount of PARV in muscle correlates with muscle fibre contraction velocity (Celio and Heizmann, 1982), which is primarily determined by myosin heavy chain isoforms (Bottinelli et al., 1991) and other myofibrillar proteins. Rapid curtailment of the Ca^{2+} signal by removal of Ca^{2+} from the sarcoplasm can increase the rate of relaxation. PARV assists this by sequestering sarcoplasmic Ca^{2+} post-contraction until it is pumped back into the SR by SR Ca^{2+}ATPase. The functional importance of this role is highlighted by the observation that a reduction in the amount of PARV in a fast-twitch muscle slows down the rate of relaxation (Klug et al., 1988) while increased PARV levels increase the rate of relaxation in the anterior fast-twitch muscle of barbel (Huriaux et al., 1997), largemouth bass (Thys et al., 2001) and trout (Coughlin et al., 2007).

Force production is related to Ca^{2+} concentration (Kerrick and Donaldson, 1975; Rome et al., 1996): the amount of Ca^{2+} available to bind troponin C correlates with the number of crossbridges that can be formed. PARV is a strong Ca^{2+} buffer and, as such, affects both the shape and size of the Ca^{2+} transient (Wnuk et al., 1982; Pauls et al., 1996). A lower PARV content may not only reduce the rate of relaxation but also facilitate an increase in the intensity of the Ca^{2+} signal, so contributing to the increase in muscle force production. Rodnick and Sidell concluded that lower amounts of PARV in the muscles of larger fish allow longer contraction durations, in turn permitting the generation of higher forces (Rodnick and Sidell, 1995). Posterior myotomes in the atlantic cod are able to maintain tension significantly longer than the anterior myotomes (Davies et al., 1995). Furthermore, longer contraction durations in the posterior myotomes of blue fin tuna contribute to the overlapping of contractions on both sides of the body, thus increasing stiffness and permitting a more effective transfer of power from the anterior musculature to the water (Wardle et al., 1989).

The functional significance of the variation in PARV isoform expression is more difficult to interpret. The isoforms that are increased in the anterior of carp fast-twitch muscle (isoforms β4 and β5) come from a different subclade to the dominant subclade (isoforms β1 and β6; Fig. 3). Isoform β4 shows very high homology to β2, and although it exhibits a lower degree of homology, β5 lies closer to β2 than to the β1/6 subclade. Inferring the functional consequences of sequence similarity is complicated. Sequence alignment reveals that there is a high degree of homology within the Ca^{2+} binding domains (CD and EF domains) with the Ca^{2+} binding residues (Kumar et al., 1990) completely conserved. The sequence differences between isoforms are mainly located within the N-terminal AB domain. However, changes in the AB domain have been shown to affect the calcium affinities of CD and EF binding sites (Permyakov et al., 1991). To date only a single study has reported the Ca^{2+} affinity of the individual isoforms (Iio and Hoshihara, 1984) as opposed to the Ca^{2+} affinity of the entire PARV fraction, which has been reported extensively (Benzonan et al., 1972; Moeschler et al., 1980; Erickson et al., 2005). This study determined the Ca^{2+} affinity of isoforms β1, β2 and β6. Isoforms β1 and β6 were found to have similar Ca^{2+} affinities, presumably corresponding to the high degree of homology observed in their sequences. Isoform β2 was found to have a Ca^{2+} affinity almost an order of magnitude higher than that of isoforms β1 and β6. Isoforms β4 and β5 belong to the same subclade as β2. Based on this evidence, it seems sensible to infer that they would have similar Ca^{2+} affinities. Therefore, any change in their expression levels is likely to have a significant effect on cellular calcium levels, despite their relatively low abundance.

In conclusion we report, in common carp, increased expression of PARV in the anterior region compared with the posterior region, especially of isoforms β4 and β5. This is accompanied by faster contraction kinetics in the anterior region. From the evidence of a previous study we hypothesise that isoforms β4 and β5 have a higher Ca^{2+} affinity relative to the other isoforms, so although the change is slight it will have a significant effect on the properties of the muscle. In addition, the posterior myotomes produced greater force. Lower concentrations of PARV in the posterior region may contribute to the generation of higher forces, which other studies have postulated may help transfer power produced in the anterior myotomes to the tail.

This study, correlating transcriptome, protein expression and physiological output demonstrates the efficacy of an integrative multidisciplinary approach for bridging the gap between genome and phenotype, but it also highlights the complexity of inter-relating mechanisms and molecular associations in a living organism. The large number of PARV isoforms and our observation of changes in isoform composition correlated with muscle function suggest a complex mechanism for the fine control of cellular Ca^{2+} handling that warrants further investigation.

LIST OF ABBREVIATIONS

ESI	electrospray ionisation
EST	expressed sequence tag
IPG	immobilised pH gradient
MALDI	matrix assisted laser desorption ionisation
MS	mass spectrometry
MS/MS	tandem mass spectrometry
m/z	mass to charge ratio
TOF	time of flight

The work was supported by the Biotechnology and Biological Sciences Research Council (BBSRC).

REFERENCES

Altringham, J. D. and Ellerby, D. J. (1999). Fish swimming: patterns in muscle function. *J. Exp. Biol.* **202**, 3397-3403.
Altringham, J. D., Wardle, C. S. and Smith, C. I. (1993). Myotomal muscle function at different locations in the body of a swimming fish. *J. Exp. Biol.* **182**, 191-206.
Baylor, S. M. and Hollingworth, S. (1998). Model of sarcomeric Ca^{2+} movements, including ATP Ca^{2+} binding and diffusion, during activation of frog skeletal muscle. *J. Gen. Physiol.* **112**, 297-316.
Benzonan, G., Capony, J. P. and Pechere, J. F. (1972). Binding of calcium to muscular parvalbumins. *Biochim. Biophys. Acta* **278**, 110-116.
Beynon, R. J. (2005). A simple tool for drawing proteolytic peptide maps. *Bioinformatics* **21**, 674-675.
Bland, J. M. and Altman, D. G. (1995). Statistics notes: multiple significance tests: the Bonferroni method. *Br. Med. J.* **310**, 170.
Bottinelli, R., Schiaffino, S. and Reggiani, C. (1991). Force-velocity relations and myosin heavy-chain isoform compositions of skinned fibers from Rat Skeletal-Muscle. *J. Physiol. (Lond.)* **437**, 655-672.
Brandts, J. F., Brennan, M. and Lin, L. N. (1977). Unfolding and refolding occur much faster for a proline-free protein than for most proline-containing proteins. *Proc. Natl. Acad. Sci. USA* **74**, 4178-4181.
Candiano, G., Bruschi, M., Musante, L., Santucci, L., Ghiggeri, G. M., Carnemolla, B., Orecchia, P., Zardi, L. and Righetti, P. G. (2004). Blue silver: a very sensitive colloidal Coomassie G-250 staining for proteome analysis. *Electrophoresis* **25**, 1327-1333.
Carver, T. and Bleasby, A. (2003). The design of Jemboss: a graphical user interface to EMBOSS. *Bioinformatics* **19**, 1837-1843.
Celio, M. R. and Heizmann, C. W. (1982). Calcium-binding protein parvalbumin is associated with fast contracting muscle-fibers. *Nature* **297**, 504-506.
Clamp, M., Cuff, J., Searle, S. M. and Barton, G. J. (2004). The Jalview Java alignment editor. *Bioinformatics* **20**, 426-427.
Clark, M. S., Edwards, Y. J. K., Peterson, D., Clifton, S. W., Thompson, A. J., Sasaki, M., Suzuki, Y., Kikuchi, K., Watabe, S., Kawakami, K. et al. (2003). Fugu ESTs: new resources for transcription analysis and genome annotation. *Genome Res.* **13**, 2747-2753.
Coffee, C. J. and Bradshaw, R. A. (1973). Carp muscle calcium-binding protein.1. characterization of tryptic peptides and complete amino-acid sequence of component-B. *J. Biol. Chem.* **248**, 3305-3312.
Coffee, C. J., Bradshaw, R. A. and Kretsinger, R. H. (1974). The coordination of calcium ions by carp muscle calcium binding proteins A, B and C. *Adv. Exp. Med. Biol.* **48**, 211-233.
Coughlin, D. J., Solomon, S. and Wilwert, J. L. (2007). Parvalbumin expression in trout swimming muscle correlates with relaxation rate. *Comp. Biochem. Physiol., Part A Mol. Integr. Physiol.* **147**, 1074-1082.
Davies, M. L. F., Johnston, I. A. and Vandewal, J. (1995). Muscle-fibers in rostral and caudal myotomes of the atlantic cod (*Gadus-morhua L*) have different mechanical-properties. *Physiol. Zool.* **68**, 673-697.
Ellerby, D. J. and Altringham, J. D. (2001). Spatial variation in fast muscle function of the rainbow trout *Oncorhynchus mykiss* during fast-starts and sprinting. *J. Exp. Biol.* **204**, 2239-2250.
Erickson, J. R., Sidell, B. D. and Moerland, T. S. (2005). Temperature sensitivity of calcium binding for parvalbumins from Antarctic and temperate zone teleost fishes. *Comp. Biochem. Physiol., Part A Mol. Integr. Physiol.* **140**, 179-185.
Felsenstein, J. (1989). PHYLIP-Phylogeny Inference Package (Version 3.2). *Cladistics* **5**, 164-166.
Friedberg, F. (2005). Parvalbumin isoforms in zebrafish. *Mol. Biol. Rep.* **32**, 167-175.
Gracey, A. Y., Fraser, E. J., Li, W. Z., Fang, Y. X., Taylor, R. R., Rogers, J., Brass, A. and Cossins, A. R. (2004). Coping with cold: an integrative, multitissue analysis of the transcriptome of a poikilothermic vertebrate. *Proc. Natl. Acad. Sci. USA* **101**, 16970-16975.
Grzyb, K. and Skorkowski, E. F. (2005). Characterization of creatine kinase isoforms in herring (*Clupea harengus*) skeletal muscle. *Comp. Biochem. Physiol. B, Biochem. Mol. Biol.* **140**, 629-634.

Henzl, M. T., Agah, S. and Larson, J. D. (2004). Rat alpha- and beta-parvalbumins: comparison of their pentacarboxylate and site-interconversion variants. *Biochemistry* **43**, 9307-9319.
Hsiao, C. D., Tsai, W. Y. and Tsai, H. J. (2002). Isolation and expression of two zebrafish homologues of parvalbumin genes related to chicken CPV3 and mammalian oncomodulin. *Mech. Dev.* **119**, S161-S166.
Huriaux, F., Collin, S., Vandewalle, P., Philippart, J. C. and Focant, B. (1997). Characterization of parvalbumin isotypes in white muscle from the barbel and expression during development. *J. Fish Biol.* **50**, 821-836.
Iio, T. and Hoshihara, Y. (1984). Static and kinetic-studies on carp muscle parvalbumins. *J. Biochem.* **96**, 321-328.
Jiang, Y., Johnson, J. D. and Rall, J. A. (1996). Parvalbumin relaxes frog skeletal muscle when sarcoplasmic reticulum Ca^{2+}-ATPase is inhibited. *Am. J. Physiol., Cell Physiol.* **39**, C411-C417.
Kerrick, W. G. L. and Donaldson, S. K. B. (1975). Comparative effects of [Ca^{2+}] and [Mg^{2+}] on tension generation in fibers of skinned frog skeletal-muscle and mechanically disrupted rat ventricular cardiac-muscle. *Pflugers Arch.* **358**, 195-201.
Klug, G. A., Leberer, E., Leisner, E., Simoneau, J. A. and Pette, D. (1988). Relationship between parvalbumin content and the speed of relaxation in chronically stimulated rabbit fast-twitch muscle. *Pflugers Arch.* **411**, 126-131.
Kumar, V. D., Lee, L. and Edwards, B. F. P. (1990). Refined crystal-structure of calcium-liganded carp parvalbumin 4.25 at 1.5-Å resolution. *Biochemistry* **29**, 1404-1412.
Lannergren, J., Elzinga, G. and Stienen, G. J. M. (1993). Force relaxation, labile heat and parvalbumin content of skeletal-muscle fibers of *Xenopus-laevis*. *J. Physiol. (Lond.)* **463**, 123-140.
Mclean, L., Young, I. S., Doherty, M. K., Robertson, D. H. L., Cossins, A. R., Gracey, A. Y., Beynon, R. J. and Whitfield, P. D. (2007). Global cooling: cold acclimation and the expression of soluble proteins in carp skeletal muscle. *Proteomics* **7**, 2667-2681.
Moeschler, H. J., Schaer, J. J. and Cox, J. A. (1980). A thermodynamic analysis of the binding of calcium and magnesium-ions to parvalbumin. *Eur. J. Biochem.* **111**, 73-78.
Muntener, M., Kaser, L., Weber, J. and Berchtold, M. W. (1995). Increase of skeletal-muscle relaxation speed by direct-injection of parvalbumin cDNA. *Proc. Natl. Acad. Sci. USA* **92**, 6504-6508.
Pauls, T. L., Durussel, I., Clark, I. D., Szabo, A. G., Berchtold, M. W. and Cox, J. A. (1996). Site-specific replacement of amino acid residues in the CD site of rat parvalbumin changes the metal specificity of this Ca^{2+}/Mg^{2+}-mixed site toward a Ca^{2+}-specific site. *Eur. J. Biochem.* **242**, 249-255.
Pechere, J. F., Demaille, J. and Capony, J. P. (1971). Muscular parvalbumins-preparative and analytical methods of general applicability. *Biochim. Biophys. Acta* **236**, 391-408.
Perkins, D. N., Pappin, D. J. C., Creasy, D. M. and Cottrell, J. S. (1999). Probability-based protein identification by searching sequence databases using mass spectrometry data. *Electrophoresis* **20**, 3551-3567.
Permyakov, E. A., Medvedkin, V. N., Mitin, Y. V. and Kretsinger, R. H. (1991). Noncovalent complex between domain AB and domains CD*EF of parvalbumin. *Biochim. Biophys. Acta* **1076**, 67-70.
Rasband, W. S. (1997-2007). ImageJ. http://rsb.info.nih.gov/ij/.
Rodnick, K. J. and Sidell, B. D. (1995). Effects of body-size and thermal-acclimation on parvalbumin concentration in white muscle of striped bass. *J. Exp. Zool.* **272**, 266-274.
Rome, L. C., Syme, D. A., Hollingworth, S., Lindstedt, S. L. and Baylor, S. M. (1996). The whistle and the rattle: the design of sound producing muscles. *Proc. Natl. Acad. Sci. USA* **93**, 8095-8100.
Schwaller, B., Dick, J., Dhoot, G., Carroll, S., Vrbova, G., Nicotera, P., Pette, D., Wyss, A., Bluethmann, H., Hunziker, W. et al. (1999). Prolonged contraction-relaxation cycle of fast-twitch muscles in parvalbumin knockout mice. *Am. J. Physiol., Cell Physiol.* **276**, C395-C403.
Swank, D. M., Zhang, G. X. and Rome, L. C. (1997). Contraction kinetics of red muscle in scup: Mechanism for variation in relaxation rate along the length of the fish. *J. Exp. Biol.* **200**, 1297-1307.
Thompson, J. D., Higgins, D. G. and Gibson, T. J. (1994). Clustal-W-improving the sensitivity of progressive multiple sequence alignment through sequence weighting, position-specific gap penalties and weight matrix choice. *Nucleic Acids Res.* **22**, 4673-4680.
Thys, T. M., Blank, J. M. and Schachat, F. H. (1998). Rostral-caudal variation in troponin T and parvalbumin correlates with differences in relaxation rates of cod axial muscle. *J. Exp. Biol.* **201**, 2993-3001.
Thys, T. M., Blank, J. M., Coughlin, D. J. and Schachat, F. (2001). Longitudinal variation in muscle protein expression and contraction kinetics of largemouth bass axial muscle. *J. Exp. Biol.* **204**, 4249-4257.
Verrez-Bagnis, V., Ladrat, C., Morzel, M., Noel, J. and Fleurence, J. (2001). Protein changes in post mortem sea bass (*Dicentrarchus labrax*) muscle monitored by one- and two-dimensional gel electrophoresis. *Electrophoresis* **22**, 1539-1544.
Vornanen, M., Tiitu, V., Kakela, R. and Aho, E. (1999). Effects of thermal acclimation on the relaxation system of crucian carp white myotomal muscle. *J. Exp. Zool.* **284**, 241-251.
Wardle, C. S., Videler, J. J., Arimoto, T., Franco, J. M. and He, P. (1989). The muscle twitch and the maximum swimming speed of giant bluefin tuna, *Thunnus-thynnus*. *J. Fish Biol.* **35**, 129-137.
Wilwert, J. L., Madhoun, N. M. and Coughlin, D. J. (2006). Parvalbumin correlates with relaxation rate in the swimming muscle of sheepshead and kingfish. *J. Exp. Biol.* **209** (2), 227-237.
Winnard, P., Cashon, R. E., Sidell, B. D. and Vayda, M. E. (2003). Isolation, characterization and nucleotide sequence of the muscle isoforms of creatine kinase from the Antarctic teleost *Chaenocephalus aceratus*. *Comp. Biochem. Physiol. B, Biochem. Mol. Biol.* **134**, 651-667.
Wnuk, W., Cox, J. A. and Stein, E. A. (1982). Parvalbumins and other soluble high-affinity calcium-binding proteins from muscle In *Calcium and Cell Function*, vol. 2 (ed. W. Y. Cheung), pp. 243-278. New York: Academic Press.